

# Cryogen Spray Cooling in Laser Dermatology: Effects of Ambient Humidity and Frost Formation

Boris Majaron, PhD,<sup>1,2</sup> Sol Kimel, PhD,<sup>1,3</sup> Wim Verkrusse, PhD,<sup>1</sup> Guillermo Aguilar, PhD,<sup>1,4,5</sup> Karl Pope, MS,<sup>6</sup> Lars O. Syaasand, PhD,<sup>1,7</sup> Enrique J. Lavernia, PhD,<sup>4,5</sup> and J. Stuart Nelson, MD, PhD<sup>1,5\*</sup>

<sup>1</sup>Beckman Laser Institute and Medical Clinic, University of California, Irvine, CA 92612

<sup>2</sup>Jožef Stefan Institute, Ljubljana, Slovenia

<sup>3</sup>Department of Chemistry, Technion—Israel Institute of Technology, Haifa 32000, Israel

<sup>4</sup>Department of Chemical and Biochemical Engineering and Materials Sciences, University of California, Irvine, CA 92697

<sup>5</sup>Whitaker Center for Biomedical Engineering, University of California, Irvine, CA 92697

<sup>6</sup>Candela Corporation, Wayland, MA 01778

<sup>7</sup>The Norwegian University of Science and Technology, Trondheim, Norway

**Background and Objective:** Dynamics of cryogen spray deposition, water condensation and frost formation is studied in relationship to cooling rate and efficiency of cryogen spray cooling (CSC) in combination with laser dermatologic surgery.

**Study Design/Materials and Methods:** A high-speed video camera was used to image the surface of human skin during and after CSC using a commercial device. The influence of ambient humidity on heat extraction dynamics was measured in an atmosphere-controlled chamber using an epoxy block with embedded thermocouples.

**Results:** A layer of liquid cryogen may remain on the skin after the spurt termination and prolong the cooling time well beyond that selected by the user. A layer of frost starts forming only after the liquid cryogen retracts. Condensation of ambient water vapor and subsequent frost formation deposit latent heat to the target site and may significantly impair the CSC cooling rate.

**Conclusion:** Frost formation following CSC does not usually affect laser dosage delivered for therapy of sub-surface targets. Moreover, frost formation may reduce the risk of cryo-injury associated with prolonged cooling. The epidermal protection during CSC assisted laser dermatologic surgery can be further improved by eliminating the adverse influence of ambient humidity. *Lasers Surg. Med.* 28:469–476, 2001. © 2001 Wiley-Liss, Inc.

**Key words:** cryo-injury; dynamic cooling; laser hair removal; port wine stain; thermal injury; threshold for epidermal damage

## INTRODUCTION

Cooling has become an integral part of the emerging discipline of laser dermatologic surgery. The novel method of achieving selective epidermal protection, with “dynamic” or cryogen spray cooling (CSC) is well established and being used for laser treatment of selected dermatoses [1–7]. CSC provides an unparalleled safety margin with

respect to prevention of undesirable epidermal injury by the laser pulse. Consequently, higher light dosages compared to laser treatment without CSC can be used, leading to more effective laser therapy in fewer treatment sessions without adverse effects.

CSC promotes rapid and spatially selective cooling of the epidermis without affecting the target chromophore temperature. Spraying human skin with cryogen will typically reduce the temperature at the skin surface to about  $-30^{\circ}\text{C}$ , whereas the temperature of the epidermal basal layer will not drop below  $0^{\circ}\text{C}$  [8]. The cryogen spurt duration ( $\tau_{\text{spurt}}$ ) and the delay between spurt termination and the laser pulse ( $\tau_{\text{delay}}$ ) can be controlled electronically, which results in reproducible cooling with predictable spatial selectivity. Pre-cooling is used to reduce the epidermal temperature before firing the laser. Parallel cooling occurs during the laser pulse and is effective if the laser pulse duration ( $\tau_{\text{pulse}}$ ) is comparable to the time necessary for the heat to diffuse out of the epidermal layer (50–100 ms) [9]. Finally, continued cooling after laser irradiation (post-cooling) reduces the time the epidermis remains at elevated temperatures, thus minimizing deleterious thermally initiated biophysical and biochemical processes.

For practical implementation of cooling in clinical management of patients receiving laser therapy, the following distinction should be made: (1) for superficial target chromophores, (e.g., port-wine stain blood vessels and dermal collagen in non-ablative skin rejuvenation) a large temperature gradient at the skin surface is required which can be achieved by CSC using short cryogen spurts and delay times; and (2) for deeper target chromophores (e.g., hair follicles) prolonged cooling times are permissible.

\*Correspondence to: J. Stuart Nelson, Beckman Laser Institute and Medical Clinic, 1002 Health Sciences Road East, Irvine, CA 92612-1475. E-mail: snelson@laser.bli.uci.edu; or: Boris Majaron, Jožef Stefan Institute, Jamova 39, SI-1000 Ljubljana, Slovenia. E-mail: boris.majaron@ijs.si.

Accepted 24 October 2000.

Although CSC in conjunction with laser therapy has become the clinical standard for several dermatologic indications, some controversy still surrounds this methodology. Recently, concerns have been raised with respect to possible adverse effects such as: (1) scattering of incident laser light by frost formation on the skin surface; and (2) risk of frostbite due to aggressive low-temperature cooling of the skin during CSC. We present herewith our studies of cryogen deposition and frost formation dynamics in relationship with cooling rate and efficiency of CSC for laser dermatologic surgery.

## MATERIALS AND METHODS

The cryogen of choice for laser dermatological indications is 1,1,1,2-tetrafluoroethane ( $C_2H_2F_4$  or R-134a; DuPont, Wilmington, DE) on the basis of the following considerations: (1) its low boiling point ( $-26^\circ C$ ) that establishes a large temperature gradient at the skin surface; (2) its relatively high latent heat of vaporization (117 J/g) to sustain evaporative epidermal cooling; (3) its adhesion to the skin to maintain good surface contact; and (4) it is non-toxic, approved by the U.S. Food and Drug Administration (FDA), and can be purchased in a medical grade formulation. Moreover, R-134a complies with the Montreal Protocol and the FDA directive on replacement of chlorofluorocarbons, which are known to deplete atmospheric ozone and contribute to global heating, as commercial refrigerants [10].

Upon release from the pressurized container (at room-temperature saturation pressure  $\sim 6.7$  bar) through an electronically controlled solenoid valve, bulk liquid cryogen is atomized into a fine spray (Fig. 1) by two mechanisms. First, vapor bubbles grow throughout the jet, as a portion of the liquid rapidly vaporizes to establish thermodynamic equilibrium ("flash evaporation"). Second, as the fluid flow is forced through the nozzle, it disintegrates due to interfacial tension and shearing forces, which strip off fine ligaments and droplets. As a result of further evaporation during the flight to the skin surface, spray droplets decrease in size and cool rapidly. Their tempera-

ture when impinging on the skin surface is typically around  $-50^\circ C$ , depending primarily on the atomizer nozzle design [11–13], and distance to the skin surface [12–17].

The spray nozzle was oriented perpendicularly to the skin surface at a distance of 35 mm. Note that cryogen was confined to the target site on the skin surface by a plastic ring attached to the laser delivery hand-piece (see Fig. 2). Upon deposition, the main cooling mechanisms of CSC is cryogen evaporation, which extracts heat from the substrate.

A high-speed video camera (Encore, Olympus America, Strongsville, OH) was used to record the spray pattern from the Candela cryogen spray nozzle. The camera was recording 1000 frames per second with a shutter speed of 1/20,000 seconds. The laser used for human skin irradiation was GentleLASE<sup>TM</sup> (Candela Laser Corporation, Wayland MA) with a wavelength of 755 nm, pulse duration  $\tau_{\text{pulse}} = 3$  milliseconds, and delivering  $14 \text{ J/cm}^2$  in a 10-mm diameter spot.

The influence of ambient humidity on heat extraction dynamics during and following CSC was monitored by spraying an epoxy block (medium viscosity, RBC Industries, Warwick, RI) with embedded thermocouples (type E, Omega Engineering, Stamford, CT; bead diameter  $90 \mu\text{m}$ ), similar to that used in earlier studies [11,15,18]. The center of the superficial thermocouples was  $90 \pm 10 \mu\text{m}$  below the sprayed surface, as determined using an optical microscope calibrated with an epoxy slab of known thickness. A deeper thermocouple was located at an approximate depth of  $250 \mu\text{m}$ . Thermocouple readings were acquired using an A/D converter board and dedicated software (InstruNet, Omega Engineering, Stamford, CT) at a sampling rate of 500 Hz and 1 millisecond integration time. The setup was enclosed in a chamber, in which humidity was varied (between the ambient value of 43% down to 7% relative humidity) by flushing with dry air or pure nitrogen gas. In this part of the study, we used a custom cryogen spray device with a nozzle similar to that in the Candela device (0.69 mm diameter, 31.7 mm length) [11].

## RESULTS

We present video images at selected time points for three different CSC regimes (Table I): (1) cooling only; (2) pre- and parallel-cooling; and (3) pre-, parallel- and post-cooling.

Figure 2 shows images of human skin in response to an 80 milliseconds cryogen spurt (Regime 1). Figures 2a and 2b display images before and during (at time  $t = 30$  milliseconds) the spurt. Figure 2b clearly shows indentation of the skin due to mechanical impact of high-velocity cryogen droplets, which undergo evaporation when striking the "hot" ( $30^\circ C$ ) skin surface. The temperature of the epidermis is rapidly reduced as it is supplying the latent heat of cryogen evaporation. As the skin temperature decreases, the heat flux becomes insufficient to vaporize the impinging droplets. At this stage, cryogen begins to accumulate on the skin surface forming a liquid layer.

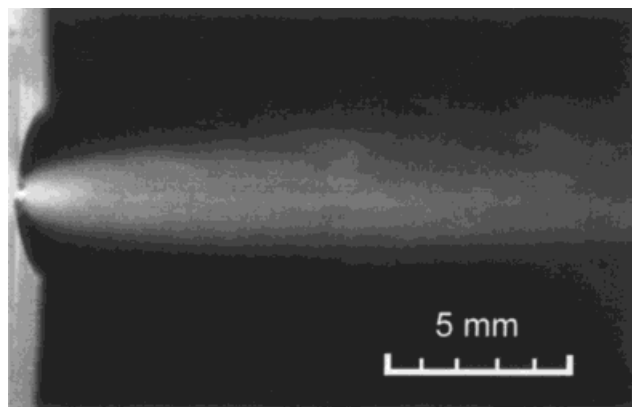


Fig. 1. Fast-flashlamp photograph of the finely atomized cryogen spray from a GentleLASE<sup>TM</sup> device (Candela Laser, Wayland, MA).

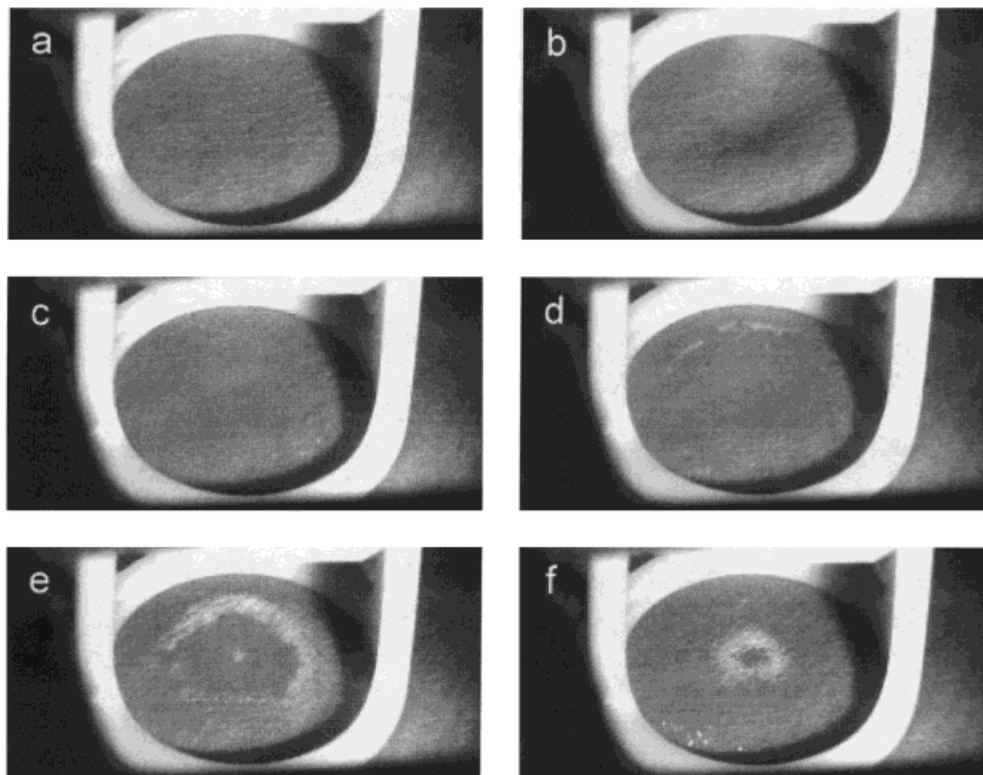


Fig. 2. Images of human skin (forearm) during CSC with an 80-millisecond cryogen spurt. Images were obtained at times (a)  $t = 0$ ; (b)  $t = 30$  milliseconds; (c)  $t = 130$  milliseconds; (d)  $t = 180$  milliseconds; (e)  $t = 230$  milliseconds and (f)  $t = 580$  milliseconds. Note indentation of liquid surface (b), appearance of frost as a ring (d), and in central area (e). See text for details.

Figure 2c shows such a “pool” of boiling cryogen on the skin surface 50 milliseconds after spurt termination ( $t = 130$  milliseconds). The temperature of this layer approaches the boiling temperature of the cryogen ( $-26^{\circ}\text{C}$ ).

Initially, vigorous evaporation of cryogen prevents the ambient air from coming in contact with the skin surface. However, as the pool of quiescent liquid cryogen reduces in area due to evaporation, a ring of cold skin is exposed to the surrounding atmosphere, which contains water vapor (<3 volume percent) that condenses to snow. In the presented example, condensation starts approximately 100 milliseconds after cryogen spurt termination (Fig. 2d,  $t = \tau_{\text{spurt}} + 100$  milliseconds). The ring is initially observed at the peripheral edges of the target site but gradually contracts toward the center as the cryogen pool continues to retract (Fig. 2e,  $t = \tau_{\text{spurt}} + 150$  milliseconds). In the next phase, a cryogen-snow slush is likely to form and slow sublimation of snow is observed (Fig. 2f, at  $t = \tau_{\text{spurt}} + 500$  milliseconds). The long residence time results from the high latent heat of sublimation (2,280 J/g) and the small temperature gradient at the skin surface. The temperature of the slush is determined by the relative quantities of cryogen and snow.

Figure 3 shows images of human skin in response to an 80 millisecond cryogen spurt, followed (after  $\tau_{\text{delay}}$ ) by

laser irradiation (Regime 2, see Table I). Figures 3a and 3b show the skin surface prior to ( $t = 140$  milliseconds) and during laser irradiation ( $t = 150$  milliseconds). After laser exposure, the liquid cryogen layer evaporates more rapidly as compared to Regime 1, due to absorption of laser energy and consequent heat generation in the epidermis. In Figure 3c, 20 milliseconds after laser irradiation ( $t = 170$  milliseconds), frost is seen to cover the entire target area; the frost persists for 400 milliseconds (until  $t = 480$  milliseconds, Fig. 3d), as compared with 500 milliseconds when the laser was not used.

Figure 4 shows images of human skin in response to a cryogen spurt, followed by laser irradiation and a second cryogen spurt immediately after the laser pulse (Regime 3). Figures 4a and 4b depict images at  $t = 600$  and 2,030 milliseconds, respectively. The post-laser cryogen spurt prolongs the presence of the liquid layer to 1,800 milliseconds, because the second spurt impinges onto a cold skin surface so that cryogen evaporation is much slower than after the first spurt. It is important to note that the hand-piece ring confines the liquid cryogen and permits the layer to build up at increased thickness.

Figure 5 presents temperature evolutions in the epoxy block during a prolonged cryogen spurt, as measured with thermocouples embedded at depths of  $90\mu\text{m}$  (comparable

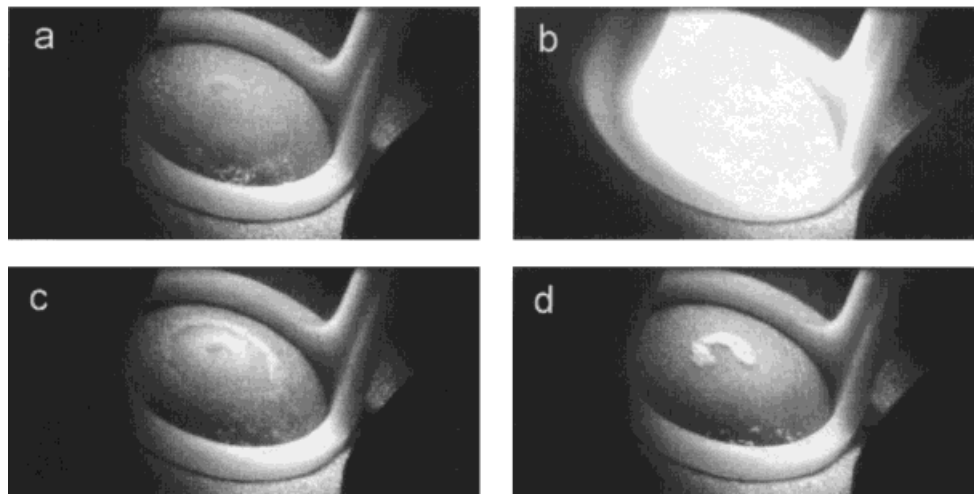


Fig. 3. Pre- and parallel cooling of human skin (forearm) sprayed with an 80-millisecond cryogen spurt. The laser pulse was delivered to the sprayed area 70 milliseconds after the spurt termination. Images were obtained at times (a)  $t = 140$ ;

(b)  $t = 150$  milliseconds, (c)  $t = 170$  milliseconds, and (d)  $t = 480$  milliseconds. Note the laser pulse (b), appearance of frost in central area (c) and sublimation (d). See text for details.

to that of the epidermal basal layer) and  $250\mu\text{m}$ . The relative humidity ( $w$ ) inside the chamber was varied in four steps between 7% (“dry air”, curve a) and the ambient value ( $w = 43\%$ , curve d). Even at a rather low humidity level of 24% (curve c), the temperature after 100 milliseconds of CSC is  $9.3^\circ\text{C}$  higher than in dry air ( $-11.5^\circ\text{C}$  vs.  $-20.8^\circ\text{C}$ ). At moderate humidity ( $w = 43\%$ , curve d), the difference is even larger and is readily observable after spraying for only 30–40 milliseconds. These results demonstrate that deposition of latent heat due to condensation (and possibly freezing) of atmospheric water on the sprayed surface influences the heat balance during CSC, and adversely affects the cooling rate and efficiency even at spurt durations shorter than 100 milliseconds.

Figure 6a presents temperature evolutions during the first second of a 3 second long cryogen spurt in dry air ( $w = 7\%$ ), as acquired simultaneously from three thermocouples embedded in the epoxy block. Data from two shallow thermocouples ( $z = 90\mu\text{m}$ ), separated laterally by several mm (curves 1, 2), indicate rather uniform cooling across the sprayed area. The temperatures decrease throughout the duration of the spurt (to  $-49^\circ\text{C}$ ), and start increasing almost immediately after its termination

(not shown in the figure). A thin layer of frost which occasionally formed on the sprayed surface was quickly blown away by the impinging cryogen droplets.

When the same measurement was performed under ambient conditions (relative humidity  $w = 43\%$ ), a significantly thicker layer of frost was formed, and particles of snow were repeatedly blown away. This is indicated also by the temperature evolution in Figure 6b (curve 1). Condensation and freezing of ambient water is depositing latent heat to the sprayed epoxy block, markedly diminishing the cooling efficiency. After the frost layer has formed, it presents a thermal insulation between the cryogen drops and the cooled surface, further impairing heat extraction from the substrate (epoxy block) and causing the temperature to stall around  $-23^\circ\text{C}$  (at  $t \sim 300$  milliseconds). The sudden drops in curve 1 (at  $t \approx 420$  and  $720$  milliseconds) indicate that the frost layer above the thermocouple was partly or completely removed, possibly exposing the substrate to the cold cryogen droplets. It is remarkable that 100–200 milliseconds after such an event, formation of a new frost layer and the corresponding latent heat deposition are so vigorous that the temperature is increasing despite continuous spraying.

TABLE 1. CSC and Laser Irradiation Conditions

Regime	Description	$\tau_{\text{spurt}}$ (milliseconds)	$\tau_{\text{delay}}$ (milliseconds)	$\tau_{\text{pulse}}$ (milliseconds)	$\tau_{\text{spurt}}$ (milliseconds)
1	Spurt	80	—	—	—
2	Spurt/delay/pulse	80	70	3	—
3	Spurt/delay/pulse/spurt	80	70	3	80

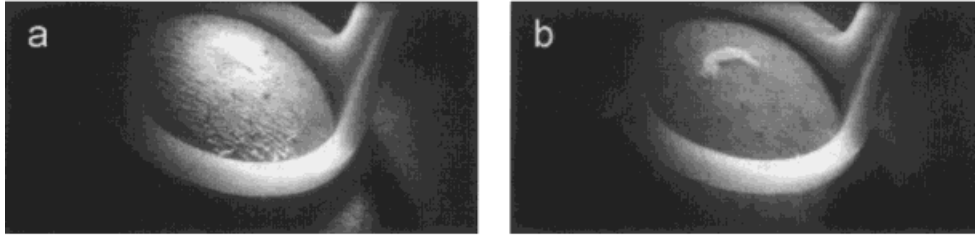


Fig. 4. Pre-, parallel- and post-cooling of human skin (forearm) sprayed with an 80 milliseconds cryogen spurt. After a delay of 70 milliseconds, a laser pulse was delivered to the sprayed area, followed by a second cryogen spurt of 80 milliseconds. Images were obtained at (a)  $t = 600$  milliseconds, and (b)  $t = 2,030$  milliseconds. See text for details.

The temperature scan from the laterally displaced thermocouple at the same depth (Fig. 6b, curve 2) essentially stalls at  $-20^{\circ}\text{C}$  (at  $t \sim 500$  milliseconds). No sudden temperature drops were observed during the 3-second long cryogen spurt, indicating lesser mechanical impact of the cryogen spray at this location. The overall adverse effect of ambient water condensation and frost formation on cooling efficiency during spraying is illustrated by the temperature measurement at a depth of  $250\mu\text{m}$  (Fig. 6b, curve 3), which is  $\sim 3^{\circ}\text{C}$  higher than in dry air after 600 milliseconds of CSC (Fig. 6a).

**DISCUSSION**

Cooling of human skin establishes a sub-surface region with lowered temperature, which reduces the epidermal temperature before, during and after laser exposure. The cooling effect persists for as long as the cryogen (or slush,

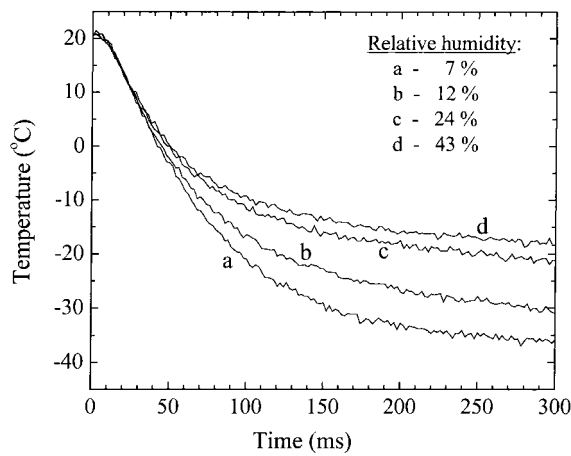


Fig. 5. Temperature evolutions in an epoxy block at depth of  $90\mu\text{m}$  during prolonged CSC at varying humidity (see the legend). Note how condensation of atmospheric water on the sprayed surface influences the cooling rate and efficiency.

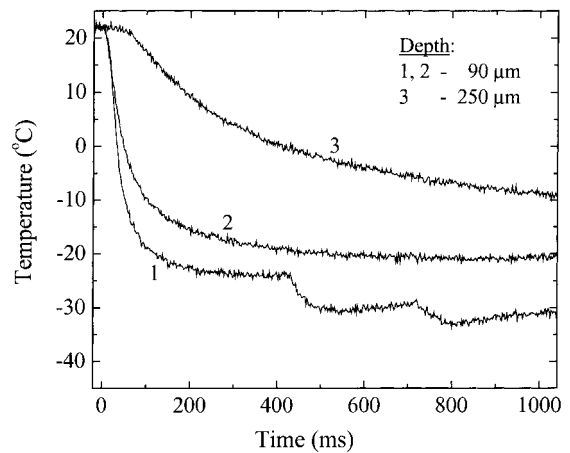
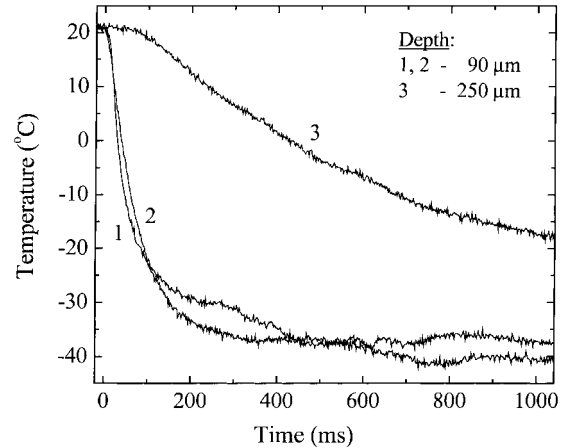


Fig. 6. (a) Temperature evolutions in an epoxy block at depths of  $90\mu\text{m}$  (curves 1, 2) and  $250\mu\text{m}$  (curve 3), during a prolonged cryogen spurt in dry air (relative humidity  $w = 7\%$ ). (b) The same measurement performed at ambient humidity ( $w = 43\%$ ) indicates a markedly diminished cooling efficiency and build-up of a thicker (thermally insulating) frost layer, which is repeatedly blown away (curve 1). Note that curves 1 and 2 deviate much more in (b) than in (a).

frost) is present on the skin surface. With CSC, a layer of liquid cryogen can remain on the skin after spurt termination (see Figs. 2 and 3). Consequently, cooling (albeit less efficient) continues for a much longer time than the user-specified cryogen spurt duration. Under these conditions, in addition to the epidermal contribution, heat conducted subsequently from dermal layers is also converted into latent heat of cryogen evaporation.

Condensation of ambient water vapor and subsequent frost formation deposit latent heat to the target site and impair the cooling rate during spraying (Figs. 5 and 6). This may have important implications for the efficiency, as well as variability of epidermal protection, depending on ambient conditions during CSC assisted laser surgery. On the other hand, due to subsequent thawing, there is no net loss of cooling efficiency over a longer period of time. For some applications, frost formation may even be beneficial, since it reduces the aggressiveness of CSC and creates a long-lasting heat sink, which helps prevent thermally initiated, time-dependent biochemical and biophysical processes that induce additional epidermal damage after laser irradiation.

Most importantly, the layer of frost starts forming only after the cryogen layer begins to retract, in the presented example approximately at  $t = \tau_{\text{spurt}} + 100$  milliseconds (Fig. 2d). Therefore, the light dosage delivered for therapy will not be affected by optical scattering due to frost, since  $\tau_{\text{delay}}$  is regularly chosen to be much shorter than 100 milliseconds (see Fig. 3a), so as to avoid losing the spatial selectivity of cooling [2,19]. (In situations where—unlike in the described Candela device—cryogen spray affects skin surface outside the treated area, such a concern would be valid with regard to delivered dosage at an adjacent, subsequently treated site. Moreover, the insulating effect of a frost layer, deposited during treatment of the previous skin site, would severely diminish the cooling rate and, consequently, spatial selectivity of CSC.)

In order to estimate the benefit of CSC with regard to epidermal injury, consider the following sample calculation. The energy per unit area ( $D_{\text{epi}}$ ) deposited or removed from the epidermis is

$$D_{\text{epi}} = \rho C d \Delta T \quad (1)$$

where  $\rho C$  denotes the specific heat per unit volume ( $3.5 \text{ J/cm}^3 \text{ K}$ ),  $d$  the epidermal thickness ( $\sim 0.1 \text{ mm}$ ), and  $\Delta T$  the temperature change in the process. Assuming that epidermal necrosis occurs when temperature in response to pulsed laser exposure exceeds  $70^\circ\text{C}$ , damage threshold corresponds to a temperature rise of  $\Delta T_{\text{dam}} = 40^\circ\text{C}$  (for initial skin surface temperature of  $30^\circ\text{C}$ ). According to (1), such temperature jump results from  $\sim 1.4 \text{ J/cm}^2$  deposited in the epidermis, which defines the threshold for its thermal injury.

Consider further that CSC reduces the temperature of human skin to about  $-30^\circ\text{C}$  and  $0^\circ\text{C}$ , at the surface and epidermal basal layer, respectively. The resulting average temperature drop in the epidermis,  $\Delta T_{\text{cryo}} = 45^\circ\text{C}$ , corresponds to an energy removal  $D_{\text{epi}} \sim 1.6 \text{ J/cm}^2$ . This more

than compensates heat deposition during the subsequent laser pulse. It is important to note that such energy removal is not simply additive to the irradiant laser dosage (fluence). Instead, it affects directly the threshold for epidermal injury. The fluence that can be safely applied without causing epidermal damage is, thus, predicted to be increased by a factor of  $(\Delta T_{\text{dam}} + \Delta T_{\text{cryo}})/\Delta T_{\text{dam}} = (40 + 45)/40 \approx 2.1$  [4]. Note that this factor is independent of the irradiation wavelength.

### Implications for laser photocoagulation of port wine stain (PWS) lesions

For PWS in Caucasian skin treated at 585–595 nm, epidermal absorption limits the total irradiant fluence, which can be applied routinely in the clinic without CSC, to about  $6\text{--}8 \text{ J/cm}^2$ . However, higher energies are required to achieve complete clearing of PWS in most patients. Further, the threshold incident dosage for epidermal injury is lower for patients with skin types III–IV, and that is where pre-cooling must be used.

Based on the above calculation, the incident fluence allowable with CSC for PWS treatment in Caucasian skin can be safely increased by a factor of 2, i.e., to  $12\text{--}16 \text{ J/cm}^2$ . Such laser dosages have been tested successfully [20,21], and are now being used routinely at BLIMC without causing epidermal damage.

For laser therapy of PWS, it is important that the effect of cooling remains spatially confined to the superficial  $100\text{--}200 \mu\text{m}$  of the skin [1,2], which requires highest achievable heat removal at its surface [19]. In that respect, the condensation of ambient water vapor and associated deposition of latent heat (Figs. 5 and 6) may limit the potential of CSC in clinical practice. Since the cooling rate is shown to vary with ambient conditions, one can in practice safely increase the delivered dose only as much as allowed in the worst possible scenario (i.e., high humidity). In this connection, a means for locally reducing the humidity around the treatment area (e.g. by blowing dry air or nitrogen gas) or verifying the actual cooling performance of the CSC device (a calibration instrument) might be a useful addition to the existing technology.

### Implications for laser hair removal (LHR)

Fluences required for effective treatment of melanin-containing hair structures 1–3 mm below the epidermis may exceed  $30 \text{ J/cm}^2$  [2,22,23]. Such high fluences pose a serious risk for epidermal thermal injury, so that cooling is as important for LHR as for PWS treatment.

In order to avoid absorption of laser light by blood, longer wavelengths ( $> 690 \text{ nm}$ ) are employed for LHR. At  $755 \text{ nm}$ , the threshold for epidermal damage is expected to be larger than at  $590 \text{ nm}$ , because the melanin absorption at  $755 \text{ nm}$  is lower as compared to  $590 \text{ nm}$  by a factor of  $(755/590)^{3.33} \approx 2.3$  [24]. Without cooling, the clinically safe fluence would thus be around  $14\text{--}18 \text{ J/cm}^2$ , whereas with CSC, it is predicted to be in the range of  $28\text{--}36 \text{ J/cm}^2$ . To this must be added the additional protection rendered by parallel- and post-cooling, so that clinical protocols using  $50 \text{ J/cm}^2$  become feasible [23].

The relatively large size of the melanin-containing target structures (0.5 mm), permits use of longer laser pulses ( $\tau_{\text{pulse}} > 20$  milliseconds), which makes pre- and parallel-cooling more efficient. For LHR, unlike in PWS treatment, cooling to 0.5–1 mm below the skin surface is permitted, and longer cooling times ( $> 500$  milliseconds) may be considered [22]. In this regard, concerns about possible cryo-injury due to deep and long-lasting temperature reductions associated with CSC must be addressed. Unfortunately, a detailed understanding is incomplete at this time, but this issue has to be analyzed before implementing longer cooling times.

Besides reducing the cooling rate, water condensation and frost formation create a long-lasting heat sink, which may help prevent thermally initiated epidermal injury at later times. When 80–100 milliseconds cryogen spurts are used with longer delays before laser irradiation ( $\tau_{\text{delay}}$ ), the temperature of the heat sink at times  $t > \tau_{\text{spurt}} + 100$  milliseconds is defined by the cryogen-snow slush rather than by liquid cryogen, so that cryo-injury is not expected and in fact has not been reported for extended post-laser cooling regimes. Spurt durations up to 100 milliseconds have frequently been used at BLIMC (albeit with shorter delay times) with no evidence of frostbite.

Finally, an advantage of CSC over other cooling modalities is its flexibility in regard to thermal interaction with the human skin. The quality of thermal contact between the cryogen drops and skin surface, expressed in terms of heat transfer coefficient ( $h$ ) ranges from 100 W/m<sup>2</sup>K for forced gas cooling to  $h = 10,000$  W/m<sup>2</sup>K or more for processes involving boiling or condensation [11,25,26]. If the risk of cryo-injury turns out to be a serious limitation, one could diminish the aggressiveness of CSC by increasing the distance between the cryogen nozzle and the skin surface [13]. This reduces the density, size and velocity of the spray droplets, resulting in lower values of  $h$ . Values as low as  $\sim 100$  W/m<sup>2</sup>K were measured at extreme distances, where only a cold mixture of air and cryogen vapor hits the skin [13].

## CONCLUSIONS

A layer of liquid cryogen may remain on the skin surface after the spurt termination and prolong the cooling time well beyond that selected by the user. Condensation of ambient water vapor and subsequent frost formation deposit latent heat to the target site, which impairs the cooling rate, but may also reduce the risk of cryo-injury associated with prolonged cooling. Frost starts forming only after the liquid cryogen layer retracts, and does usually not affect the laser dosage delivered for therapy. In conclusion, the extent and lateral homogeneity of epidermal protection during CSC assisted laser dermatologic surgery can be further improved by reducing the adverse influence of ambient humidity.

## ACKNOWLEDGMENTS

This project was supported by a research grant awarded from the Institute of Arthritis and Musculoskeletal and Skin Diseases (AR43419) at the National Institutes of

Health to J. S. Nelson. A research grant from Candela Corporation (482560-59109 to E. J. Lavernia and J. S. Nelson) and institutional support from the Office of Naval Research, Department of Energy, National Institutes of Health and the Beckman Laser Institute and Medical Clinic Endowment is also acknowledged. B. Majaron is supported in part by the Slovenian Ministry of Science and Technology. The methodology described in this manuscript is contained within United States Patent Number 5,814,040—Apparatus and Method for Dynamic Cooling of Biological Tissues for Thermal Mediated Surgery—awarded to J.S. Nelson, M.D., Ph.D., T. E. Milner, Ph.D. and L. O. Svaasand, Ph.D. and assigned to the Regents of the University of California.

## REFERENCES

1. Nelson JS, Milner TE, Anvari B, Tanenbaum BS, Kimel S, Svaasand LO, Jacques SL. Dynamic epidermal cooling during pulsed laser treatment of port-wine stain. *Arch Dermatol* 1995;131:695–700.
2. Nelson JS, Milner TE, Anvari B, Tanenbaum BS, Svaasand LO, Kimel S. Dynamic epidermal cooling in conjunction with laser-induced photothermolysis of port wine stain blood vessels. *Lasers Surg Med* 1996;19:224–229.
3. Waldorf HA, Alster TS, McMillan K, Kauvar ANB, Geronemus RG, Nelson JS. Effect of dynamic cooling on 585 nm pulsed dye laser treatment of port wine stain birthmarks. *Dermatol Surg* 1997;23:657–662.
4. Chang CJ, Nelson JS. Cryogen spray cooling and higher fluence pulsed dye laser treatment improve port wine stain clearance while minimizing epidermal damage. *Dermatol Surg* 1999; 25: 767–772.
5. Kelly KM, Nelson JS, Lask GP, Geronemus RG, Bernstein LJ. Cryogen spray cooling in combination with non-ablative laser treatment of facial rhytides. *Arch Dermatol* 1999;135: 691–694.
6. Fiskerstrand EJ, Norvang LT, Svaasand LO. Laser treatment of port-wine stains: reduced pain and shorter duration of purpura by epidermal cooling. *Proc SPIE* 1996;2922:20–28.
7. Nelson JS, Majaron B, Kelly KM. Active skin cooling in conjunction with laser dermatologic surgery: methodology and clinical results. *Semin Cutan Med Surg* 2000;19:253–266.
8. Pope K, Lask G. Epidermal temperature evaluation during dynamic spray cooling, contact cooling, and ice. Presented at the 20th Annual meeting of the ASLMS, Reno, NV, April 2000.
9. Zenzie HH, Altshuler GB, Smirnov MZ, Anderson RR. Evaluation of cooling methods for laser dermatology. *Lasers Surg Med* 2000;26:130–144.
10. Kanakidou M, Dentener FJ, Crutzen PJ. A global three-dimensional study of the fate of HCFCs and HFC-134a in the troposphere. *J Geophys Res* 1995;100:18781–18801.
11. Verkruysse W, Majaron B, Aguilar G, Svaasand LO, Nelson JS. Dynamics of cryogen deposition relative to heat extraction rate during cryogen spray cooling. *Proc SPIE* 2000;3907: 37–48.
12. Aguilar G, Majaron B, Verkruysse W, Nelson JS, Lavernia EJ. Characterization of cryogenic spray nozzles with application to skin cooling. (Internat. Mechanical Engineering Congress, Orlando, FL, Nov. 2000) *Proc ASME* 2000;253: 189–197.
13. Aguilar G, Majaron B, Pope K, Svaasand LO, Lavernia EJ, Nelson JS. Determination of optimum nozzle-to-skin distance for cryogen spray nozzles used in laser dermatology. *Lasers Surg Med* 2001;28:113–120.
14. Anvari B, Ver Steeg BJ, Milner TE, Tanenbaum BS, Klein TJ, Gerstner E, Kimel S, Nelson JS. Cryogen spray cooling of human skin: effects of ambient humidity level, spraying distance, and cryogen boiling point. *Proc. SPIE* 1997;3192: 106–110.

15. Torres JH, Anvari B, Tanenbaum BS, Milner TE, Yu, JC, Nelson JS. Internal temperature measurements in response to cryogen spray cooling of a skin phantom. *Proc SPIE* 1999; 3590:11–19.
16. Aguilar G, Verkruysse W, Majaron B, Zhou Y, Nelson JS, Lavernia EJ. Modeling of cryogenic spray temperature and evaporation rate based on single-droplet analysis. *Proc ICLASS 2000*; 1004-1009. 8th Internat. Conf. on Liquid Atomization and Spray Systems, Pasadena, CA, July 2000.
17. Aguilar G, Majaron B, Verkruysse W, Zhou Y, Nelson JS, Lavernia EJ. Theoretical and experimental analysis of droplet diameter, temperature, and evaporation rate evolution in cryogenic sprays. *Int J Heat Mass Tran* (in press).
18. Torres JH, Nelson JS, Tanenbaum BS, Milner TE, Goodman DM, Anvari B. Estimation of internal skin temperature measurements in response to cryogen spray cooling: implications for laser therapy of port wine stains. *IEEE J Special Topics Quant Elect* 1999;5:1058–1066.
19. Verkruysse W, Majaron B, Tanenbaum BS, Nelson JS. Optimal cryogen spray cooling parameters for pulsed laser treatment of port wine stains. *Lasers Med Surg* 2000;27:165–170.
20. Kelly KM, Nanda VS, Shirin S, Nelson JS. Vascular lesion treatment utilizing a pulsed dye laser at high fluences in combination with cryogen spray cooling. *Lasers Surg Med* 2000; Supp. 12: 24.
21. Kauvar ANB, Lou WW, Zelickson B. Effect of cryogen spray cooling on 595 nm, 1.5 ms pulsed dye laser treatment of port wine stains. *Lasers Surg Med* 2000; Supp.12: 24.
22. Ross EV, Ladin Z, Kreindel M, Dierickx C. Theoretical considerations in laser hair removal. *Dermatol Clinics* 1999; 17:333–355.
23. Rohrer TE, Touma DJ, Ugent SJ, Goldberg LJ, Lavine C. Evaluating the 3 millisecond alexandrite laser with a tetrafluoroethane cooling spray for hair removal. *Arch Dermatol* (in press).
24. Meglinsky IV, Matcher SJ. The determination of absorption coefficient of skin melanin in visible and NIR spectral region. *Proc SPIE* 2000; 3907: 143–150.
25. Incropera FP, DeWitt DP. *Fundamentals of Heat and Mass Transfer*, 4th edn. New York: John Wiley and Sons, 1996, p. 8.
26. Svaasand LO, Randeberg LL, Aguilar G, Verkruyse W, Majaron B, Kimel S, Lavernia EJ, Nelson JS, Berns MW. Technique for measuring the heat transfer coefficient during cryogen spray cooling of human skin. Submitted to *J. Biomed. Engineering*.